A Facile Solution-Doping Method to Improve a Low-Temperature Zinc Oxide Precursor: Towards Low-Cost Electronics on Plastic Foil

Dennis Weber, Silviu Botnaraș,* Duy Vu Pham, Alexey Merkulov, Jürgen Steiger, Roland Schmechel, and Luisa De Cola*

Optimization of thin-film transistors performance is usually accompanied by an increase of the process temperature. This work presents a method to raise the field effect mobility by a factor of 3 without a change of the process parameters. The modification involves a solution doping process where an ammine zinc complex is formed in the presence of metal ions of the 13th group, namely gallium and indium. Morphological studies, including scanning electron microscopy and atomic force microscopy, reveal the difference among the resulting films. Moreover, X-ray diffraction results show that the doping affects the preferred orientation of the zinc oxide crystals in the resulting film. The electrical properties vary distinctly and are best for a solution doped with both gallium and indium. With a double-layer system the performance of this new precursor exceeds field effect mobility values of 1 cm^2 V^{-1} s^{-1} after a maximum process temperature of 160 °C.

1. Introduction

It is a common agreement that metal oxide semiconductors are facing a bright future in the field of thin-film transistors (TFTs).[1–5] During an era of research, metal oxides were promised to fulfill a range of demands: Facile processing, increased electrical performance, low prices, broader fields of application, etc.[1–3,6,7] Among these claims a lowering of the process temperature while maintaining a device performance comparable to amorphous silicon (≈1 cm^2 V^{-1} s^{-1}) is of special interest; the term low-temperature high-performance is prevalent in TFT related publications.[6,8–10] Different plastic foils are the substrates of choice for many research groups.[8,11] It allows the production of flexible and lightweight devices, durability as well as low-price fabrication.[12,13] Simplified, it could be stated that the price of the substrate increases with tolerance towards heat. Examples for the upper end of the price range are PI (polyimide) and PEEK (polyether ether ketone) which allow the highest process temperatures of up to 250 °C.[13,14] For low-cost applications the heat treatment must be reduced to 150 °C or 120 °C for PEN (polyethylene naphthalate) or PET (polyethylene terephthalate), respectively.

The routes towards this goal are numerous. Vacuum techniques, especially sputtering, offer deposition at room temperature.[11] Yet, a subsequent annealing step is required to ensure sufficient performance and, more importantly, electrical stability.[6] On the other hand are the solution processes. They can be divided into two methods. Coating inks can be generated by the dispersion of metal oxide nanoparticles or the application of precursor solutions with subsequent conversion into metal oxides.[2,6,15] While the first approach suffers from the large amount of grain boundaries the latter usually requires high temperature treatments or other drastic procedures.[9,16,17]

Publications about solution processed metal oxide TFTs have gained a lot of attention in the last few years, and the interest is growing. Several recent review articles cover some of the approaches.[6,9] Current examples of routes towards low-temperature processes include a combustion method.[18] The reduction of the annealing temperature is achieved by adding an oxidizer (NO_3^-) and a fuel (acetylacetone or urea) to the precursor solution. Thermogravimetric analyses showed the effectiveness of this approach and device performance was realized after heat treatments as low as 200 °C; corresponding to a reduction of up to 100 °C compared to the conventional precursor. Another path is the activation of sol-gel reactions by UV irradiation—and partly by subsequent vacuum treatment.[19–21] With these methods the thermal exposure was reduced to temperatures as low as 135 °C. Device fabrication has also been proven on PAR-foil, however, this high-tech polymer does not meet the requirement of low-cost preparation. A more simple method has been published by Meyers et al.[22] By employing an

D. Weber
Physikalisches Institut and Center for Nanotechnology
Heisenbergstr. 11, 48149, Münster, Germany
E-mail: d_webe06@uni-muenster.de
Dr. S. Botnaraș, Prof. R. Schmechel
Faculty of Engineering and Center for Nanointegration Duisburg-Essen (CeNIDE)
University Duisburg-Essen
Carl-Benz-Str. 199, 47057, Duisburg, Germany
E-mail: silviu.botnaras@stud.uni-due.de
D. Weber, Dr. S. Botnaraș, Dr. D. V. Pham, Dr. A. Merkulov, Dr. J. Steiger
Coatings & Additives, Evonik Industries AG
Paul-Baumann-Str., 1, 45764, Marl, Germany
Prof. L. De Cola
Institut de Science et d'Ingénierie Supramoléculaires (I.S.I.S.)
Université de Strasbourg
8 allée Gaspard Monge, 67000, Strasbourg, France

DOI: 10.1002/adfm.201303461

ammonium solution of zinc hydroxide they realized mobility values of 0.4 $cm^2 V^{-1} s^{-1}$. The annealing takes place at 150 °C making it suitable to be applied on PEN-foil.

By a facile doping method it is possible to increase the performance of the latter precursor even further. Surprisingly, this can be achieved by doping the solution with small amounts (<1%) of metal ions of the 13th group, species which are considered insoluble in aqueous ammonia. The generated ink is converted at a maximum process temperature of 160 °C, a procedure that allows the transfer to PEN foil. The effect of the solution doping on the film morphology as well as the device performance of thin-film transistors is described in this work.

2. Chemistry of the Precursor

The chemistry of aqueous ammine-hydroxo zinc complexes are described in detail in the initial publication by Meyers and co-workers.[22] The main advantages of this system are worth noting, namely the lability and high volatility of ammine ligands which make this precursor especially suitable for low temperature processes. In contrast to a wide variety of metal-organic approaches the all-inorganic zinc complex requires little energy for the hydroxo-condensation. Hydroxide formation is followed by dehydration and oxide crystallization at temperatures below 100 °C. In addition, the aqueous system is free of carbon atoms which are hard to remove from resulting films.

Jun et al. achieved the incorporation of yttrium into the solution which results in more stable electrical characteristics.[23] Jung et al. developed this method further by co-doping with lithium and zirconium.[24] However, these doped formulations require higher temperatures since dehydration of the dopants takes place at ≈300 °C and ≈250 °C, respectively. Cho et al. incorporated zinc oxide nanoparticles into the formulation that contained the described ammine-hydroxo complex of zinc and thereby improved the field effect mobility to 0.9 $cm^2 V^{-1} s^{-1}$ at a maximum process temperature of 150 °C.[25] On the other hand, mixed oxides containing zinc and group 13 elements (e.g., In-Ga-ZnO) have raised a lot of interest lately. However, the chemistry of aqueous ammonia solutions is so particular that it is not an option to generate films of mixed metal oxides by the described method. In fact, hydroxides of the third main group are amphoteric, hence risk to be discarded after the first centrifugation step along with sodium hydroxide: while $Ga(OH)_3$ readily forms the corresponding tetrahydroxide anion, $[Ga(OH)_4]^-$, indium requires highly basic conditions to form indate ions. In addition, these hydroxides convert into their respective metal oxide at temperatures much higher than 300 °C. In summary, the chemistry of these species in the high pH range varies strongly from zinc and conversion requires drastic conditions.

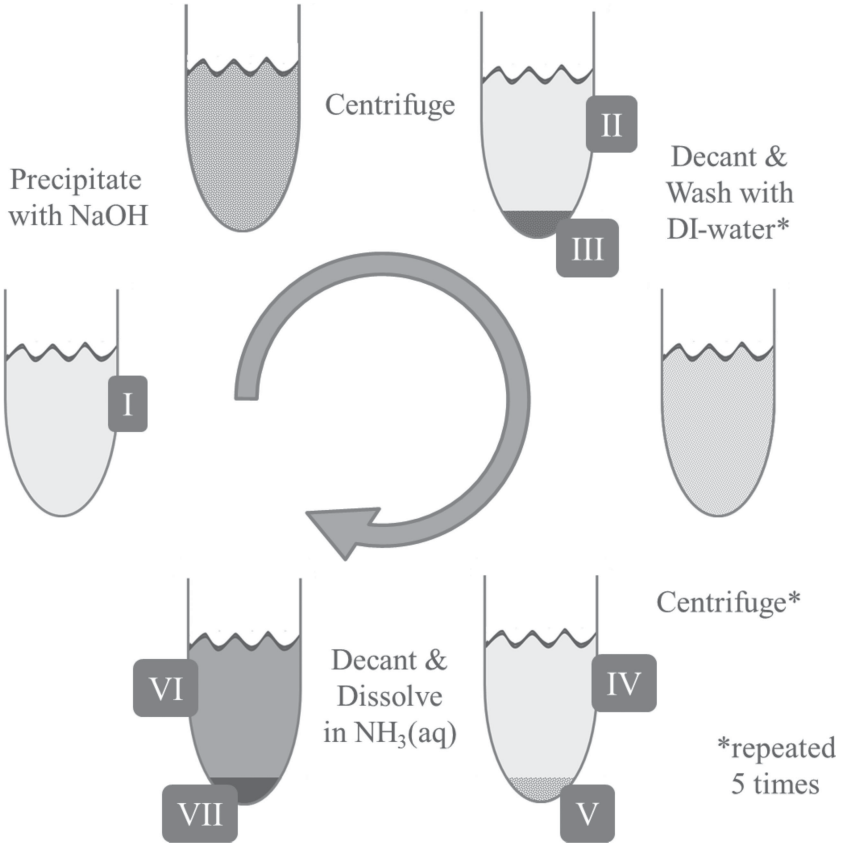

Figure 1. Schematic representation of the solution-doping process. The roman numbers indicate different components that were analyzed by ICP-AES (Table S1, Supporting Information).

3. Results and Discussion

3.1. Synthesis and Analysis of the Precursor

In order to generate a doped formulation a zinc nitrate solution containing the dopants, gallium and/or indium nitrate/s, is precipitated with $NaOH_{(aq)}$. The precipitate can then be rinsed with DI-water to remove the sodium ions. Finally, the precipitate is dissolved in aqueous ammonia to obtain the ink; the insoluble part is left to sediment. The process flow is summarized schematically in **Figure 1**. It is worth noting that the resulting formulation is a saturated solution. A detailed study on the presence of the ions by in inductively coupled plasma atomic emission spectroscopy (ICP-AES) (Table S1, Supporting information) reveals: 1) Zinc hydroxide forms the matrix (III), only small amounts re-dissolve in the supernatant (II) and little is removed during the washing steps (IV). With more than 99% of the ion content it is the major species in the final ink (VI). 2) The amphoteric nature of gallium hydroxide is evident; it is detected in the precipitate (III) as well as in the sodium hydroxide solution (II). It is also removed to a notable degree by the washing procedure (IV). The ink (VI) contains detectable traces of gallium ions. It mostly remains in the undissolved precipitate (VII) of the final formulation. 3) Indium is not detectable in any of the solutions, neither in the sodium hydroxide solution (II), the washing water (IV) nor

Table 1. Ion concentration of the initial nitrate solution (according to amounts weighed in) and the resulting formulation (ICP-AES). And the respective film composition according to GDMS analysis. Note that the latter method is used rather qualitatively and no precise percentage values were obtained (no standard available).

	Zn^{2+} in ZnO	Ga^{3+} in ZnO	In^{3+} in ZnO	Zn^{2+} in ZnO:Ga	Ga^{3+} in ZnO:Ga	In^{3+} in ZnO:Ga	Zn^{2+} in ZnO:Ga,In	Ga^{3+} in ZnO:Ga,In	In^{3+} in ZnO:Ga,In
Initial ratio	100%	0%	0%	70%	30%	0%	66.5%	28.5%	5%
Ink	100%	<10 ppm[a)]	<5 ppm[a)]	99.9%	0.1%	<5 ppm[a)]	99.8%	0.2%	<5 ppm[a)]
Film	>99.99%	<0.01%	- [b)]	>99.93%	< 0.07%	- [b)]	>99.35%	<0.65%	- [b)]

[a)]Below detection limit; [b)]Not detected, detection limit unknown.

in the final formulation (VI). The indium hydroxide remains in the precipitate (III, V and VII) over the course of synthesis, also when subjected to the ammonium hydroxide solution. 4) The amount of sodium is decreased by the washing procedure, trace amounts remain.

Since the concentration of the dopants is low an increase in conversion temperature is not expected. One would assume that adding small amounts of the dopants in form of their nitrates would suffice; however, the ratios of group 13 metal nitrates before precipitation (solution I) need to be in a range of several percent in order to obtain the desired effect. The best results were obtained for initial ratios of Zn/Ga/In of 0.665/0.285/0.05. In the final formulation (VI) the ratio of gallium is reduced to a value below 1% while the presence of indium ions cannot be confirmed by ICP-AES, **Table 1** summarizes the metal ion concentrations in the solutions prepared by the described method. The loss of large amounts of the dopants is certainly a drawback and further research will be directed at a recycling process. The hydroxides could for example be separated and dried to the respective oxides which could be used for different purposes.[26,27]

The solutions are labeled according to the ions that were incorporated: ZnO includes no further ions except zinc, ZnO:Ga was synthesized with zinc and gallium nitrate and ZnO:Ga,In was made by precipitating the nitrates of zinc, gallium, as well as indium. Since the final ink contains small or non-detectable amounts of the added ions the term doping refers to the solution.

3.2. Thin Film Morphology

The insight into the chemistry does not yet explain how the trace amounts will lead to an improvement in the electrical performance of thin-film transistors. Apart from the material (for example, its composition), the film morphology is a major factor that determines the performance.[3,6] Interface effects as well as crystallinity, preferred orientation and the grain size have a strong influence on the charge transport.[28–33]

Since the added ions of the 13th group are present only in traces their abundance in the resulting oxide films is expected to be low. Analyses of the film compositions by glow discharge mass spectrometry (GDMS) proved this assumption; indium ions were not detectable while gallium ions were found in trace amounts. Table 1 includes the results of the respective film compositions, the individual mass spectra are displayed in Figure S1 (Supporting Information).

Studies on the film morphology were performed by SEM; the images of **Figure 2** (left column) show a notable difference. However, the samples prepared with the doped solutions have a much rougher surface which usually leads to a poorer device performance. Another notable difference is the film thickness of the resulting zinc oxide layer; spectroscopic ellipsometry revealed values ranging from 21 nm (ZnO) and 28 nm (ZnO:Ga) to roughly 40 nm (ZnO:Ga,In). This is surprising since the ICP-AES analysis shows only a small variation in metal ion concentration (Table S2, Supporting Information), in fact, the undoped solution has the highest metal ion content.

More insight has been gained by atomic force microscopy, especially when the phase image was studied. The increasing roughness is verified in the topography mode (Figure 2 middle column), the respective area roughness values (S_q, root mean squared) are 1.44 nm for ZnO, 2.27 nm for ZnO:Ga and 4.66 nm for ZnO:Ga,In. However, the phase contrast (Figure 2, right column) reveals that the solution doping leads to an increase in the average grain size. This could also explain the same trend in the film thickness; if the crystals grow in size not only 2-dimensionally but rather 3-dimensionally it will result in a thicker film. The reason for this finding is not yet fully understood. A possible explanation could be an inhibited nucleation of zinc oxide by the doping. Particle growth thereby becomes dominant and results in larger grains.

Multiple coatings of the solution allowed the analysis of the films by powder X-ray diffraction; the film thickness was adjusted to 200 nm for all samples. To suppress the influence and especially the reflexes from the substrate the samples were prepared on thin microscope cover glasses. **Figure 3** shows the respective X-ray diffractograms of films made with ZnO, ZnO:Ga and ZnO:Ga,In inks. The black lines are the fitted data; fast Fourier transform was used to smoothen the diffractograms. The most prominent effect is the growth of the (002) reflex at 34.4° from ZnO over ZnO:Ga to ZnO:Ga,In. It is missing in the first case, apart from a small hump indicating its position, and grows to become the predominant feature for samples made with ZnO:Ga,In. At the same time the intensities of the reflexes at 31.8° (100) and 36.2° (101) decrease in a similar manner. In the case of films made with ZnO:Ga,In their position is only indicated by small humps. The positions of the reflexes coincide with the values reported for zinc oxide in the literature.[34] The orientation is reported to have a strong influence on the electron mobility and it is stated that c-axis orientation along the (002) plane is preferred.[22,32]

The orientation of solution-processed zinc oxide is reported to depend strongly on the annealing temperature. Ong et al.

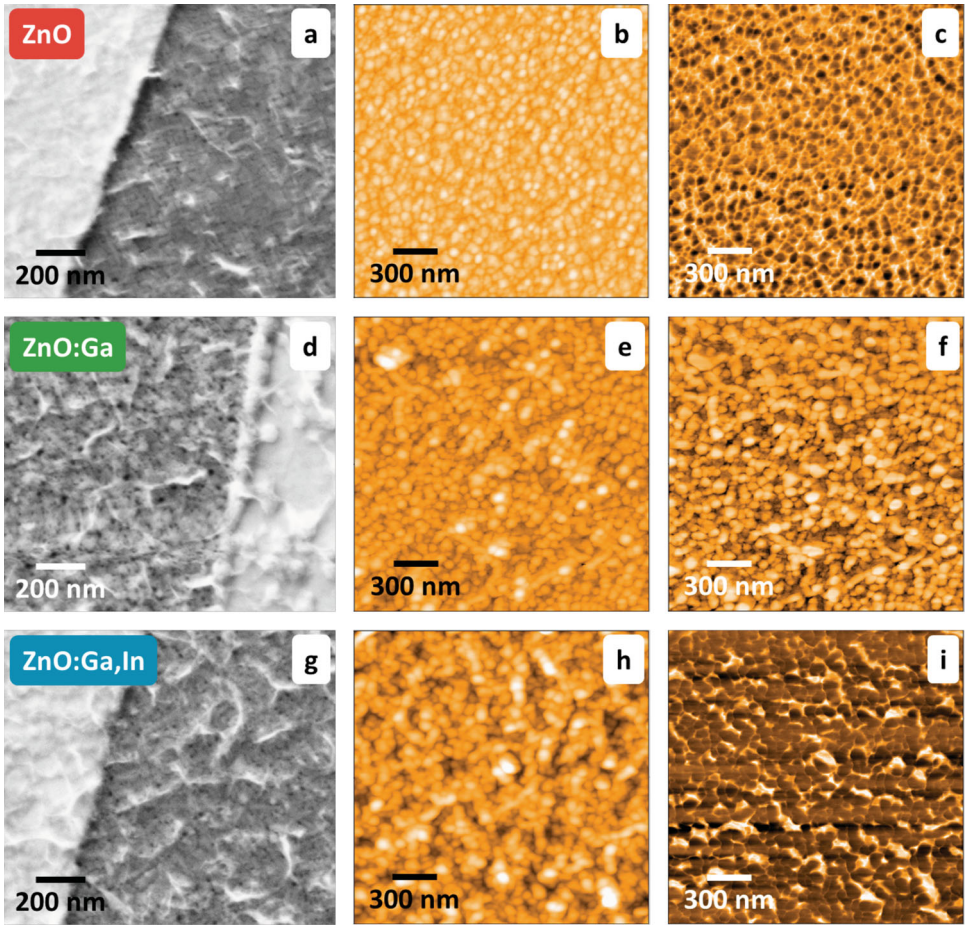

Figure 2. a,d,g) SEM micrographs and b,e,h) AFM images of the topography, and c,f,i) phase contrast. The respective samples were prepared with ZnO (top row), ZnO:Ga (middle row), and ZnO:Ga,In (bottom row) inks.

showed that an instant thermal treatment of 350 °C or more results in the preferred orientation while slowly heating the samples from room temperature did not lead to this phenomenon, independent of the final temperature.[32] Also Meyers et al. observed a preferred orientation along the c-axis after annealing the samples made with the ammine-hydroxo zinc complex at temperatures larger than 300 °C.[22] Literature on the effect of dopants on the preferred orientation of the zinc oxide crystals is numerous. However, they are hardly comparable; the film formation and also the concentration ranges vary strongly from what is reported in this work. In general it is described that dopants, due to difference in their ionic radii, deter the zinc oxide structure and disturb the creation of a preferred orientation.[35,36] The solution-doping leads to much lower concentrations of the dopants, especially of indium, so that another mechanism should be envisaged. A detailed study of the crystallization phenomena would exceed the scope of this work. The results reported herein cannot shed light into the discussion about the reason for a preferred orientation discussed in the literature.[37] Nevertheless, it is assumed that nucleation phenomena are responsible for the observed effects. One of the few reports on such phenomena studied the influence of cobalt dopants on the growth of zinc oxide crystals: Bryan et al. show that the Co^{2+} ions are not incorporated in the nuclei of the crystallites; moreover, their presence impedes nucleation.[38]

3.3. Electrical Characterization

Solution doping results in a substantial difference in film morphology as well as a change of the preferred orientation of the zinc oxide films. Since the research interest is to increase the electrical performance of low-temperature ZnO-based thin-film transistors, their performance was investigated. The experiments have been carried out on Si/SiO_2 substrates with a bottom gate/bottom contact configuration. The process temperature for all samples has never exceeded 160 °C. It was found that after the annealing on a hot plate the performance can be enhanced by an additional annealing step at 160 °C under reduced pressure (200 mbar). The transfer characteristics of 3 representative solution-doped samples are shown in **Figure 4**. The non-doped sample (ZnO) reflects the results from the work of Meyers et al.[22] The other samples were prepared with a gallium-doped solution (ZnO:Ga) or with a gallium- and indium-doped ink (ZnO:Ga,In), the respective device parameters can be found in **Table 2**. The difference in the field effect

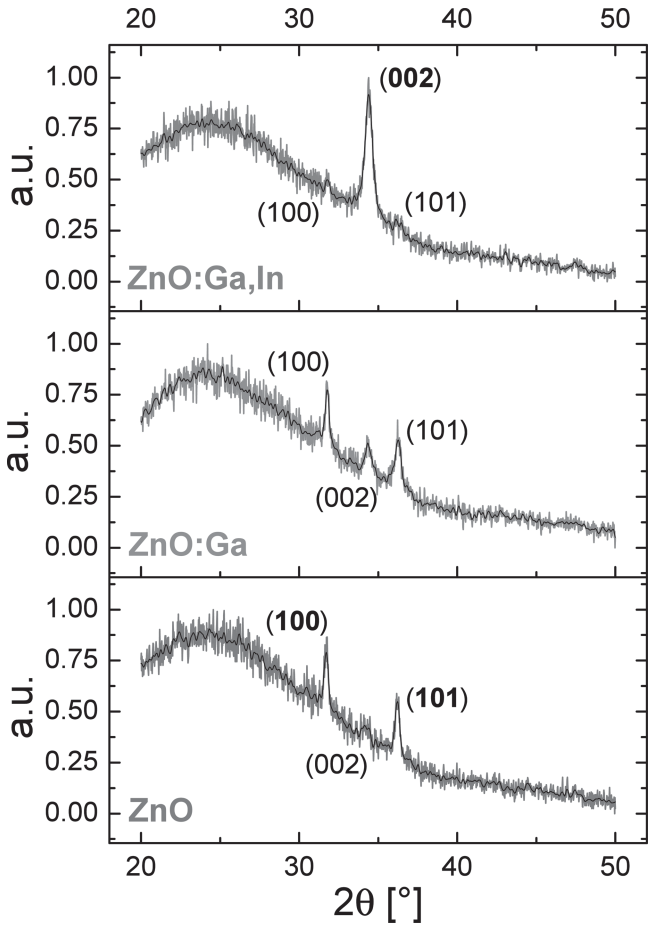

Figure 3. Normalized X-ray diffractograms of films made by multiple coating steps of different solutions on microscope cover glasses. The black line represents the respective FFT-smoothing.

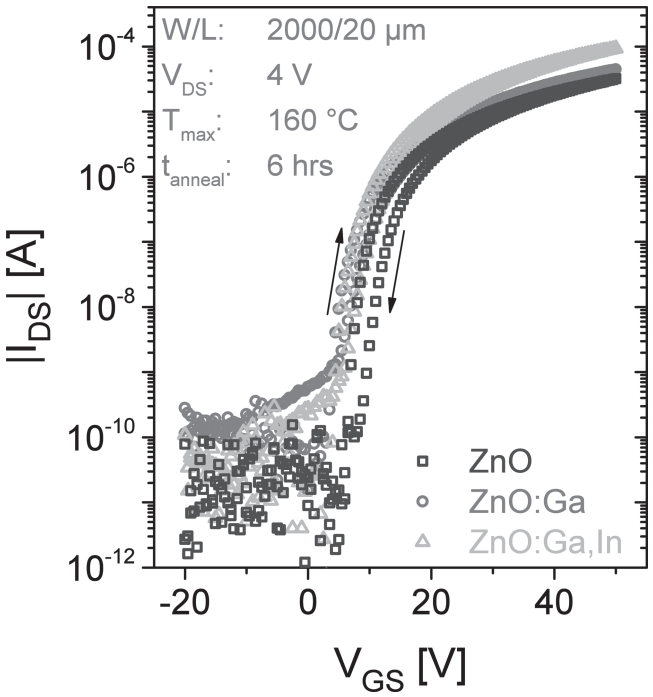

Figure 4. Transfer characteristics of representative TFTs processed with ZnO (□), ZnO:Ga (○), and ZnO:Ga,In (△) at a maximum temperature of 160 °C.

mobility values compared to Meyers´ work, 0.2 instead of 0.4 $cm^2 V^{-1} s^{-1}$, can be ascribed to the different device architecture (bottom contact vs top contact; different thickness of the dielectric)

The major effect of the addition of gallium (ZnO:Ga) is a significant shift of the turn on voltage (V_{On}) from more than 7 V to 3.5 V. Besides, the extracted field-effect mobility increases moderately, the hysteresis is reduced and the current level in the off-state is slightly raised. By adding indium to the system (ZnO:Ga,In) the improvement of V_{On} is equivalent to the gallium-doped sample. The current level in the Off-state is kept at the value of the undoped material while the on-current is further increased. This results in a larger On/Off ratio of ~10^7 and a threefold mobility value of 0.62 $cm^2 V^{-1} s^{-1}$.

To exclude that the observed phenomena is a coincident effect a series of solutions (>15) and samples (>50) has been prepared and characterized. The average values including their standard deviation are summarized in **Figure 5**. Two conclusions can be drawn from the collected data. The first is related to the preparation of the solution. If only zinc nitrate is used no variation of the composition is possible, the duration of precipitation and/or stirring have a minor influence. Hence, the performances of the resulting ZnO-based transistor do not vary largely, as indicated by the small deviation. On the other hand, if more degrees of freedom are introduced, the deviation is much broader. The preparation of the ink is more sensitive to the individual factors. The second conclusion allows to rule out a coincident effect, especially for the ZnO:Ga,In formulation. The average mobility of the latter is more than two times higher than for ZnO samples, the respective values are 0.58 $cm^2 V^{-1} s^{-1}$ and 0.24 $cm^2 V^{-1} s^{-1}$. Even the worst ZnO:Ga,In sample still shows better performance than the best ZnO sample. Table S3 (Supporting Information) offers a detailed listing of mobility values of samples prepared with the individual solutions.

Finally, to investigate the influence of the film thickness in more detail multi-layer samples have been prepared. **Figure 6** shows the evolution of performance with respect to the film thickness. The plot allows to conclude that a second layer improves the performance dramatically; however, subsequent layers only lead to a small improvement for ZnO:Ga,In and no further rise for ZnO. By this method it was possible to

Table 2. Device parameters of TFTs processed with ZnO, ZnO:Ga and ZnO:Ga,In at a maximum temperature of 160 °C.

	Turn on voltage [V]	On current [mA]	On/Off current ratio	Linear mobility [$cm^2 V^{-1} s^{-1}$]	Saturation mobility [$cm^2 V^{-1} s^{-1}$]
ZnO	7.5	0.032	5×10^6	0.21	0.16
ZnO:Ga	3.5	0.044	3×10^6	0.30	0.20
ZnO:Ga,In	4	0.093	1×10^7	0.62	0.46

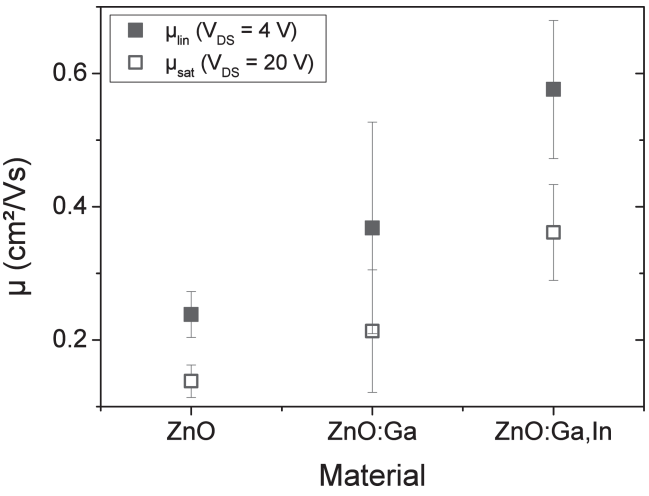

Figure 5. Average field effect mobility values and their respective standard deviation of a series of samples prepared with the different formulations, See Table S3 for details.

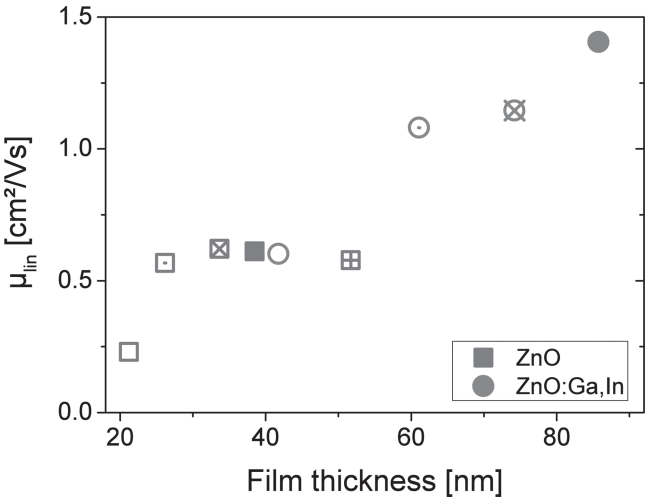

Figure 6. Influence of the film thickness obtained by multiple coating steps of undoped solution (square) and ZnO:Ga,In solution (circle). Multiple layers with intermediate annealing steps were deposited (hollow: 1 layer; dot: 2 layers; X: 3 layers; solid: 4 layers; +>4 layers).

obtain similar film thicknesses of ZnO (38.5 nm, 4 layers) and ZnO:Ga,In (41.8 nm, 1 layer). The performance is indeed comparable, but since more than 2 layers of ZnO lead to no further increase in mobility values only ZnO:Ga,In is able to deliver field effect mobility values larger than 1 $cm^2\ V^{-1}\ s^{-1}$.

4. Conclusion

To summarize, the electrical performance of solution processed zinc oxide can be raised dramatically by a simple doping procedure. Metal ions of the thirteenth group are co-precipitated together with zinc ions during the formation of the respective hydroxides. Even though most of the added metal ions were removed during the synthesis – hence the term solution-doping – their addition strongly affects the film morphology. Rougher surfaces as well as increased film thickness values were observed for samples prepared with doped solutions. The most dominant effects are the increase in grain size and the change of the preferred orientation of the crystallites obtained by the doping technique. The beneficial effect on the performance of thin-film transistors fabricated at a maximum process temperature of 160 °C is described in detail. The respective mobility values tripled by this approach; from 0.2 $cm^2\ V^{-1}\ s^{-1}$ to 0.6 $cm^2\ V^{-1}\ s^{-1}$. Increasing the film thickness by multiple spin coating steps lead to field effect mobility values of more than 1 $cm^2\ V^{-1}\ s^{-1}$ with values ranging up to 1.4 $cm^2\ V^{-1}\ s^{-1}$ (μ_{lin}) and 0.75 $cm^2\ V^{-1}\ s^{-1}$ (μ_{sat}). Rockelé et al. reported on TFTs fabricated with the material described herein on PEN foil and showed exceptional performance: mobility values (μ_{sat}) of up to 1.1 $cm^2\ V^{-1}\ s^{-1}$ were attained.[39]

5. Experimental Section

Solution Doping: All chemicals were used as received without further purification. Different ratios of zinc nitrate hexahydrate (Alfa Aesar, 99.998%), gallium(III) nitrate hydrate (Alfa Aesar, 99.999%) as well as indium(III) nitrate hydrate (Sigma Aldrich, 99.999%) were dissolved in DI-water to obtain an overall metal ion concentration of 0.5 mmol mL^{-1}. The corresponding compositions (Zn/Ga/In) were: ZnO (1/-/-), ZnO:Ga (0.7/0.3/-) and ZnO:Ga,In (0.665/0.285/0.05). Sodium hydroxide (Merck, pa) was dissolved in DI-water to give a concentration of 25 mmol mL^{-1}. 10 mL of this basic solution were added to 15 mL of the nitrate solution. The resulting slurry was stirred shortly and then centrifuged at 4500 rpm for 20 min. The supernatant was removed and the precipitate was thoroughly rinsed with 15 mL of DI-water. Again, the slurry was centrifuged and the liquid was discarded. The washing step was repeated another 4× to ensure sufficient removal of the sodium ions. The final precipitate was dissolved in ammonium hydroxide solution (Sigma Aldrich, 28 % NH_3 in H_2O, ≥ 99.99 %) to give a concentrated solution. ICP-AES analysis was performed with a Varian 720ES.

Preparation of Films: Film formation was performed by dispensing 100 µL of the ink onto UV/Ozone pre-treated bottom-gate/bottom-contact substrates. The substrates with a size of 15 mm × 15 mm were comprised of highly p-doped Silicon with a thermally grown SiO_2 layer (230 nm). Source and drain electrodes were made of 10 nm indium tin oxide (ITO) and 40 nm of gold, channel length and width were 20 µm and 2000 µm. The spin-coating parameters were 3000 rpm for 20 s with an acceleration of 10 000 rpm s^{-1}. The samples were annealed on hot plates (2 h) and subsequently treated in a vacuum oven (4 h at 200 mbar), both at 160 °C. Multi-layered samples were treated for 15 s at 160 °C on a hot plate between coating procedures. SEM as well as AFM images were recorded on TFT samples with a Zeiss 1540 EsB and a Nanosurf Mobile S, respectively. The surface roughness was extracted from the AFM images. The film thickness was determined by a spectroscopic ellipsometer, SE800 DUV from Sentech Instruments. Values were validated by AFM scans of etched edges. XRD diffractograms of films deposited on microscope cover glasses were recorded with a Rigaku Miniflex II.

Electrical Characterization: Measurements were performed in N_2-atmosphere directly after device fabrication with a Keithley 2612 sourcemeter and a Keithley 3706-NFP switch/multimeter. The transfer characteristics were fitted with Equations 1 or 2 to extract the field effect mobility; the majority of the values refer to μ_{lin}, if Equation 2 was used it is indicated throughout the text.

$$\mu_{lin} = \frac{\partial I_D}{\partial V_{GS}} \cdot \frac{L}{WC_i V_{DS}} \quad (1)$$

$$\mu_{sat} = \frac{2L}{WC_i} \cdot \left(\frac{\partial \left(\sqrt{I_D} \right)}{\partial V_{GS}} \right)^2 \quad (2)$$

L and W are the channel length and width, C_i is the dielectric constant per unit area, I_D is the drain current and V_{GS}/V_{DS} is the gate–source/drain–source voltage.

Supporting Information

Supporting Information is available from the Wiley Online Library or from the author.

Acknowledgements

The research leading to these results has received funding from the European Community's Seventh Framework Program FP7-ICT-2009–4 under Grant Agreement No. 247798 of the ORICLA project. From this program special thank is directed to Maarten Rockelé and Paul Heremanns for their work with the presented material on flexible substrates (PEN).

Received: October 8, 2013
Revised: November 5, 2013
Published online: January 6, 2014

[1] J. K. Jeong, *Semicond. Sci. Technol.* **2011**, *26*, 034008.
[2] J. S. Park, W.-J. Maeng, H.-S. Kim, J.-S. Park, *Thin Solid Films* **2012**, *520*, 1679.
[3] J. F. Wager, D. A. Keszler, R. E. Presley, Transparent Electronics, Springer, New York **2008**.
[4] K. Nomura, H. Ohta, K. Ueda, T. Kamiya, M. Hirano, H. Hosono, *Science* **2003**, *300*, 1269.
[5] A. Janotti, C. G. Van de Walle, *Rep. Prog. Phys.* **2009**, *72*, 126501.
[6] E. Fortunato, P. Barquinha, R. Martins, *Adv. Mater.* **2012**, *24*, 2945.
[7] R. Martins, E. Fortunato, P. Barquinha, L. Pereira, Transparent Electronics – From Materials to Devices, John Wiley & Sons, West Sussex **2012**.
[8] R. A. Street, *Adv. Mater.* **2009**, *21*, 2007.
[9] S. Jeong, J. Moon, *J. Mater. Chem.* **2012**, *22*, 1243.
[10] M.-G. Kim, M. G. Kanatzidis, A. Facchetti, T. J. Marks, *Nat Mater.* **2011**, *10*, 382.
[11] K. K. Banger, Y. Yamashita, K. Mori, R. L. Peterson, T. Leedham, J. Rickard, H. Sirringhaus, *Nat. Mater.* **2011**, *10*, 45.
[12] K. Nomura, H. Ohta, A. Takagi, T. Kamiya, M. Hirano, H. Hosono, *Nature* **2004**, *432*, 488.
[13] Y. Sun, J. Rogers, *Adv. Mater.* **2007**, *19*, 1897.
[14] A. Facchetti, T. J. Marks, Transparent Electronics – From Synthesis to Applications, John Wiley & Sons, West Sussex **2010**.
[15] M. Rockelé, D.-V. Pham, J. Steiger, S. Botnaras, D. Weber, J. Vanfleteren, T. Sterken, D. Cuypers, S. Steudel, K. Myny, S. Schols, B. v. der Putten, J. Genoe, P. Heremans, *J. Soc. Inf. Display* **2012**, *9*, 499.
[16] A. Bashir, P. H. Wöbkenberg, J. Smith, J. M. Ball, G. Adamopoulos, D. D. C. Bradley, T. D. Anthopoulos, *Adv. Mater.* **2009**, *21*, 2226.
[17] R. M. Pasquarelli, D. S. Ginley, R. O´Hayre, *Chem. Soc. Rev.* **2011**, *40*, 5406.
[18] D. B. Mitzi, Solution Processing of Inorganic Materials, John Wiley & Sons, New York **2009**.
[19] S.-Y. Han, G. S. Herman, C.-H. Chang, *J. Am. Chem. Soc.* **2011**, *133*, 5166.
[20] Y.-H. Kim, J.-S. Heo, T.-H. Kim, S. Park, M.-H. Yoon, J. Kim, M. S. Oh, G.-R. Yi, Y.-Y. Noh, S. K. Park, *Nature* **2012**, *489*, 128.
[21] Y. H. Hwang, S.-J. Seo, J.-H. Jeon, B.-S. Bae, *Electrochem. Solid-State Lett.* **2012**, *15*, H91.
[22] S. T. Meyers, J. T. Anderson, C. M. Hung, J. Thompson, J. F. Wager, D. A. Keszler, *J. Am. Chem. Soc.* **2008**, *130*, 17603.
[23] T. Jun, K. Song, Y. Jung, S. Jeong, J. Moon, *J. Mater. Chem.* **2011**, *21*, 13524.
[24] Y. Jung, W. Yang, C. Y. Koo, K. Song, J. Moon, *J. Mater. Chem.* **2012**, *22*, 5390.
[25] S. Y. Cho, Y. H. Kang, J.-Y. Jung, S. Y. Nam, J. Lim, S. C. Yoon, D. H. Choi, C. Lee, *Chem. Mater.* **2012**, *24*, 3517.
[26] M. Niederberger, G. Garnweitner, J. Buha, J. Polleux, J. Ba, N. Pinna, *J. Sol-Gel Sci. Technol.* **2006**, *40*, 259.
[27] M. Muruganandham, R. Amutha, M. S. M. Abdel Wahed, B. Ahmmad, Y. Kuroda, R. P. S. Sury, J. J. Wu, M. E. T. Sillanpää, *J. Phys. Chem. C* **2012**, *116*, 44.
[28] X. L. Chen, X. H. Geng, J. M. Xue, D. K. Zhang, G. F. Hou, Y. Zhao, *J. Cryst. Growth* **2006**, *296*, 43.
[29] M. S. Hammer, D. Rauh, V. Lorrmann, C. Deibel, V. Dyakonov, *Nanotechnology* **2008**, *19*, 485701.
[30] B. J. Ingram, G. B. Gonzalez, D. R. Kammler, M. I. Bertoni, T. O. Mason, *J. Electroceram.* **2004**, *13*, 167.
[31] Y. H. Hwang, S.-J. Seo, B. S. Bae, *J. Mater. Res.* **2010**, *25*, 695.
[32] B. S. Ong, C. Li, Y. Li, Y. Wu, R. Loutfy, *J. Am. Chem. Soc.* **2007**, *129*, 2750.
[33] E. Fortunato, P. Barquinha, A. Pimentel, A. Gonçalves, A. Marques, L. Pereira, R. Martins, *Thin Solid Films* **2005**, *487*, 205.
[34] J. I. Langford, A. Boultif, J. P. Auffredic, D. Louer, *J. Appl. Cryst.* **1993**, *26*, 22.
[35] Y. Morinaga, K. Sakuragi, N. Fujimura, T. Ito, *J. Cryst. Growth* **1997**, *174*, 691.
[36] J. Wienke, A. S. Booij, *Thin Solid Films* **2008**, *516*, 4508.
[37] Y. Kajikawa, *J. Cryst. Growth* **2006**, *289*, 387.
[38] J. Bryan, D. A. Schwartz, D. R. Gamelin, *J. Nanosci. Nanotechnol.* **2005**, *5*, 1472.
[39] M. Rockelé, M. Nag, T. H. Ke, S. Botnaras, D. Weber, D. V. Pham, J. Steiger, S. Steudel, K. Myny, S. Schols, B. v. der Putten, J. Genoe, P. Heremans, Proceedings of the International Display workshops, pp. 299–302, Kyoto, Japan, **2012**.